16th World Conference on Earthquake Engineering, 16WCEE 2017

Santiago Chile, January 9th to 13th 2017

Paper N° 2369

Registration Code: S-N1461835059

VERIFICATION OF DRIFT DEMANDS IN THE DESIGN OF RC BUILDINGS WITH MASONRY INFILLS

S. Hak[1], P. Morandi[2], G. Magenes[2]

[1] *Research associate, University of Zagreb, Faculty of Civil Engineering, Croatia, sanja.hak@grad.hr*
[2] *Researcher, University of Pavia, Department of Civil Engineering and Architecture & Eucentre, Italy, paolo.morandi@unipv.it*
[3] *Full professor, University of Pavia, Department of Civil Engineering and Architecture & Eucentre, Italy, guido.magenes@unipv.it*

Abstract

Given the significant influence that masonry infill typologies constructed in full contact with adjacent structural elements may have on the seismic response of RC structures, the importance of integrated verification methods, accounting for the presence of non-structural infill in the structural design phase is frequently pointed out. Nevertheless, in practice, masonry infills are regularly considered only in terms of mass and vertical loads. This choice may be justified according to European code provisions, as long as possible adverse effects such as consequences of irregularities in plan and elevation or increased local shear demands in regions of interaction are prevented.

On the other hand, calculations required to ensure the achievement of given performance objectives related to different limit states should not be limited to structural elements only, but also have to result in a satisfactory response of non-structural components. In order to limit the in-plane infill damage, inter-story drift limitations are commonly imposed in the design of RC structures. However, the commonly adopted approach, relying on the verification of bare frame drift demands against a code-defined drift limit that is independent of the building configuration and adopted infill typologies, may not always guarantee satisfactory results. Specifically, in function of the deformation capacity of the infill, expected extents of damage may not be sufficiently limited, or on the contrary overly conservative design choices, for example related to the size of structural elements, may be imposed. The careful evaluation of expected drift demands and their verification against appropriate drift limits related to the available deformation capacity is particularly important at higher levels of seismic action, for the damage control of weaker infill typologies, or in the case of building configurations with scarcely distributed infills.

The present study has focused on possible improvements regarding commonly adopted procedures for the verification of inter-story drift demands in the design of RC structures with masonry infills. In particular, the possibility to control drift demands corresponding to infilled configurations against the critical drift limit in function of the infill deformation capacity was envisaged. Therefore, a simple parameter that accounts for structural properties of the load-bearing system and quantifies the presence of different masonry infills was adopted, implying a relationship between drift demands of bare and infilled configurations. Accordingly, a simplified approach is proposed to verify the expected inter-storey drift demands of the RC building with masonry infills, based on related values for the corresponding bare configuration. To support the described procedure, results of extensive parametric studies, including nonlinear dynamic analyses of selected frame and wall-frame dual systems designed according to current European seismic code recommendations are presented and the practical application of the proposed approach is discussed in the light of current design provisions.

Keywords: masonry infills; seismic design; in-plane drift demands; RC buildings;

1. Introduction

Non-structural masonry infills erected in full contact with adjacent RC structural elements, representing a traditional construction technique, are still widely adopted in European countries, including regions of relatively high seismicity, such as Italy, Spain, Portugal or Turkey. The assessment of masonry infill damage during field surveys after earthquakes in Europe during recent years have frequently pointed to certain deficiencies in current design approaches and/or construction techniques, see *e.g.* [1], [2] and [3], revealing the need for further research efforts in the field, *e.g.* [4]. In common design practice rigid masonry infills are most frequently considered only in terms of masses and vertical loads, while analyses and safety verifications are performed on bare frame structural models. European seismic code regulations [4] do not explicitly recommend such approach, but also do not provide much space for alternatives, which would result in more sophisticated reliable, but still easily applicable design methods. Given the fact that the structural resistance has to be verified at life safety conditions, when the stiffness of weaker masonry infill typologies is expected to be substantially reduced due to extensive cracking, the choice of neglecting non-structural infills is reasonable from the practitioner's viewpoint. Additionally, the strongly non-linear response of masonry infills and the complexity of related modelling procedures, especially in the case of infills with openings, represent a strong obstacle to the introduction of practical design methodologies, which would require the explicit representation of masonry infills in the design of RC structures. Furthermore, the variety of available masonry infill typologies and construction techniques, as well as the possible variability of infill layouts during the life of the structure may lead to an additional lack of appropriate attention at different design stages.

Nevertheless, an adequate seismic response has to be ensured also for the infilled configuration and performance requirements defined for damage limitation and life safety limit states have to be fulfilled, considering not only a rational design of structural elements, but also the satisfactory response of masonry infills. Based on the response of different RC frame configurations, previous numerical investigations [6] have shown that, in terms of in-plane damage, the behavior of unreinforced masonry infill walls in RC frames designed in compliance with present European seismic code regulation [5] can result to be unsatisfactory. Regarding the limitation of infill damage, the current design approach imposes the application of a single inter-storey drift limit at the damage limitation limit state, being equal to 0.50% for the case of rigid masonry infills. A single damage control parameter, applied to the bare structure independently of the structural layout, the infill distribution and the adopted masonry typology, allows only a rough control of the actual infill damage and may not always be able to guarantee a sufficient level of safety without imposing unnecessarily oversized RC structural elements. Specifically, referring to both limit states, the current design approach may be insufficient in some cases, such as for sparse and/or weak infills having low displacement capacities. On the other hand, for densely distributed and/or enhanced infill types or innovative infill typologies with significantly increased levels of displacement capacity, overly conservative requirements may be imposed. Consequently, accounting in a simplified manner for the most significant parameters influencing the infill response can improve the infill verification procedure in terms of allowable in-plane drifts.

2 Significant parameters for the response of RC structures with masonry infills

2.1 Infill deformation capacity, stiffness and strength

In line with widely accepted numerical modelling assumptions, in particular when the global structural response is of primary interest, see *e.g.* [7], masonry infills in RC structures are commonly represented using simple single-strut models of appropriate geometrical properties (see Fig. 1a), described by a suitable nonlinear stress-strain relationship, *e.g.* [8]. The force-displacement response envelope of the infill typically includes several characteristic points, which can be assigned to different performance limit states and represented by corresponding strain parameters. Assuming that values of strain reached in the infill strut can be related to equivalent structural inter-storey drifts through simple geometric relations [9], the attainment of damage limitation and ultimate limit state conditions can be described either in terms of strain (ε_m' and ε_u) or in terms of inter-storey drift ($\delta_m' = d_m'/h$ and $\delta_u = d_u/h$, where d_m' and d_u are the related values of horizontal displacement, *h* is the storey height). Given that according to Eurocode 8 – Part 1 [5], for masonry infills both the limitation of damage and the prevention of failure have to be ensured, inter-storey drifts assigned to limit state conditions defined with reference to the masonry infill performance represent significant properties required to characterize the expected response of a specific infill typology.

Masonry infill limit states have been defined for instance through the interpretation of test results [10] for traditional unreinforced and lightly reinforced weak/slender infill typologies [9]. Similarly, in more recent studies, extensive experimental tests have been carried out for contemporary strong clay block masonry infills [11], [12], also resulting in the evaluation of limit states in function of inter-storey drift limits. A summary of inter-storey drifts corresponding to the attainment of operational, damage limitation and ultimate limit state performance requirements for different infill solutions is given in Table 1.

Table 1. Inter-storey drift limits for unreinforced masonry infills at different limit states

Limit State	**Slender/weak infills** Calvi *et al.* 2001 [10], Hak et al. 2013 [9]	**Strong infills** Morandi *et al.* 2014 [12]
Operational δ_{OLS} [%]	0.20	0.30
Damage δ_{DLS} [%]	0.30	0.50
Ultimate δ_{ULS} [%]	1.00	1.75

The stiffness of a single masonry infill within a RC structure, referring to bay i in storey j, may be approximated by means of the secant stiffness $K_{I,i,j}$, corresponding to the horizontal force $F_{w,i,j}$, reached at the displacement equal to $d_{m,i,j}$, as given in Equation 1a and illustrated in Fig. 1b. Analogously, as given in Equation 1b, where h_j denotes the storey height, the secant stiffness $K_{I,i,j}$ can be expressed in function of the inter-storey drift $\delta_{m,i,j}'$ that approximately corresponds to the associated strain $\varepsilon_{m,i,j}'$.

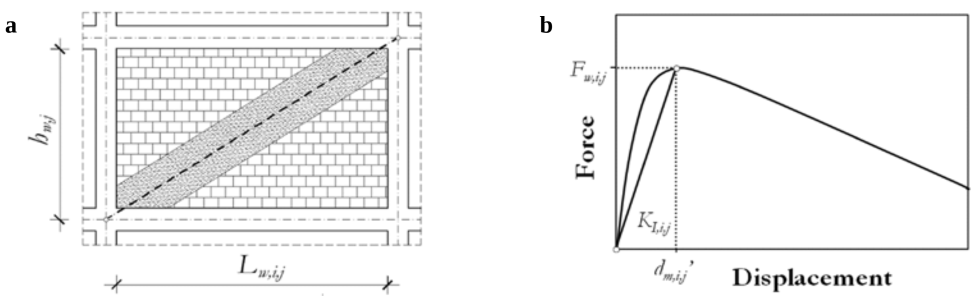

Figure 1. a) Masonry infill secant stiffness; b) Equivalent diagonal strut model

$$K_{I,i,j} = \frac{F_{w,i,j}}{d_{m,i,j}'}, \; K_{I,i,j} = \frac{F_{w,i,j}}{\delta_{m,i,j}' h_j} \tag{1a,b}$$

Considering one load-bearing direction of a frame or wall-frame dual structural system, the total stiffness $K_{I,j}$ of all infills in storey j (j = 1...n_s, where n_s is the number of storeys) can be evaluated as the sum resulting from the contribution of each single masonry infill, as given in Equations 2a and 2b, where $n_{b,j}$ is the number of bays in storey j. If for all infills in the same storey masonry typologies with equal deformation capacities ($\delta_{m,i,j}' = \delta_{m,j}'$, $i = 1 \ldots n_{b,j}$) are foreseen, the stiffness $K_{I,j}$ may be expressed by Equation 3. Similarly, if in the same storey the use of infill types with varying properties in terms of strength and deformation capacity is anticipated, the equivalent drift capacity $\delta_{m,j}'$, resulting in the same stiffness $K_{I,j}$, may be evaluated from Equation 4.

$$K_{I,j} = \sum_{i=1}^{n_{b,j}} K_{I,i,j}, \quad K_{I,j} = \frac{1}{h_j} \sum_{i=1}^{n_{b,j}} \frac{F_{w,i,j}}{\delta_{m,i,j}'} \tag{2a,b}$$

$$K_{I,j} = \frac{1}{h_j \delta_{m,j}'} \sum_{i=1}^{n_{b,j}} F_{w,i,j} \tag{3}$$

$$\delta_{m,j}' = \frac{\sum_{i=1}^{n_{b,j}} F_{w,i,j}}{\sum_{i=1}^{n_{b,j}} \frac{F_{w,i,j}}{\delta_{m,i,j}'}} \tag{4}$$

In order to achieve a suitable approximation, the horizontal force $F_{w,i,j}$ may be taken equal to the peak horizontal strength of the masonry infill, calculated according to Equation 5, where $f_{w,i,j}$ denotes the governing masonry strength, $t_{w,i,j}$ the thickness and $L_{w,i,j}$ the length for infill i in storey j.

$$F_{w,i,j} = f_{w,i,j} t_{w,i,j} L_{w,i,j} \tag{5}$$

In absence of more specific data, the masonry strength $f_{w,i,j}$ may be estimated in accordance with Eurocode 8 – Part 1 [5], on the basis of the corresponding shear strength of bed joints, which may be assumed equal to the initial shear strength under zero compressive stress $f_{v0,i,j}$. However, with the aim of being more accurate, in order to evaluate the infill strength $f_{w,i,j}$, more detailed models accounting for different infill failure modes [13] should preferably be adopted when the required data, such as the horizontal and vertical compression strength as well as the shear strength under diagonal cracking, is available. Nevertheless, such approach can be directly applied only in the case of unreinforced infills without openings. The presence of openings may influence the performance of masonry infills significantly, see e.g. [14], [15]. Therefore, in the case of realistic building configurations, the possible reduction of strength for perforated masonry infills has to be considered, as discussed in more detail in [15].

2.2 Structural stiffness

The structural layouts addressed within the scope of this study are assumed to be regular in both plan and elevation and not significantly affected by contributions from modes of vibration higher than the fundamental mode in each principal direction. Hence, torsional effects should not influence the response significantly. Therefore, it is assumed that the stiffness of the load-bearing system may be evaluated independently for two orthogonal directions.

Values of elastic stiffness assigned to each storey along the height of a RC structure can be approximated based on the elastic analysis of a bare frame structural model using the equivalent static force approach. In particular, according to Equation 9, the average elastic structural stiffness $K_{S,j}$ for storey j may be estimated as the ratio of the horizontal storey shear V_j, evaluated in line with Equation 10, n_s being the number of storeys, and the corresponding inter-storey displacement $d_{r,j}$ (*i.e.* the difference of the average lateral displacements $d_{s,j}$ and $d_{s,j-1}$ at the top and at the bottom of storey j), given in Equation 11.

$$K_{S,j} = \frac{V_j}{d_{r,j}} \tag{9}$$

$$V_j = \sum_{i=j}^{n_s} F_i \tag{10}$$

$$d_{r,j} = d_{s,j} - d_{s,j-1} \tag{11}$$

For the evaluation of the elastic structural stiffness $K_{S,j}$ per storey according to Equation 9, the distribution of horizontal forces acting along the building height is needed. The force F_j acting on storey j can for instance be determined according to Equation 12, where F_b is the total seismic shear force, s_i, s_j are the displacements of masses i and j in the fundamental mode shape, while m_i, m_j are the corresponding storey masses, associated with gravity loads, assumed in the seismic load combination. The evaluation of the seismic base shear F_b is expressed by Equation 13, where the fundamental period of vibration T_1 and the mass M_1 participating in the first mode response can be estimated from a modal analysis and $S_e(T_1)$ is the corresponding spectral ordinate of the elastic response spectrum.

$$F_j = F_b \frac{s_j \cdot m_j}{\sum_{i=1}^{n_s} s_i \cdot m_i} \tag{12}$$

$$F_b = S_e(T_1) \cdot M_1 \tag{13}$$

2.3 Average stiffness ratio

Subsequently, for each load-bearing direction of a regular RC structural configuration, given the distribution of infills and all properties required to characterize the adopted infill typologies, knowing the infill parameter $K_{I,j}$ and the structural stiffness parameter $K_{S,j}$ for each storey (j = 1...n_s, where n_s is the number of stories), the relative density-stiffness coefficient C_j can be defined, representing an average ratio of infill *vs.* structural stiffness for each storey along the building height, as given in Equation 14.)

$$C_j = \frac{K_{I,j}}{K_{S,j}} \tag{14}$$

Introducing the simplified density-stiffness coefficient C_j, the combined influence of masonry infill strength and stiffness with respect to the stiffness of the structural elements on the response of infilled RC buildings can be assessed. Therefore, the establishment of a relation between inter-storey drift demands for bare and infilled structural configurations in function of the coefficient C_j is envisaged, aimed to allow a safe-sided estimation of inter-storey drifts for the infilled structure based on the given structural layout and infill properties, knowing the inter-storey drift demands of the corresponding bare structural configuration.

3. Description of the parametric numerical investigations

3.1 Motivation and scope

Based on an extensive numerical study, see [6], [16] and [18], results of nonlinear time-history analyses for different structural layouts, infill distributions and masonry typologies have been evaluated with the aim to assess the correlation of inter-storey drift demands for bare and infilled RC structural systems. The correlation has been established in function of different properties, which can be accounted for through a unique parameter, the density-stiffness coefficient C_j given by Equation (14). The extensive analyses were carried out considering newly designed two-dimensional RC frame structures and three-dimensional frame and wall-frame dual systems meant to represent characteristic structural configurations, which can be frequently found in the European building stock. Moreover, three masonry infill typologies of increasing strength and stiffness have been assumed and variations of their distribution within the structure have been accounted for.

3.2 Prototype structural configurations

The selected case study structures included two-dimensional RC frames assumed to represent typical 5.0 m spaced internal structural planes consisting of three bays (5.0 m, 2.0 m, and 5.0 m), being part of a simple spatial structural systems with a varying number of stories, *i.e.* 3-storey, 6-storey and 9-storey buildings of 3.0 m storey height. Each frame configuration was designed for five different levels of seismicity, corresponding to design peak ground accelerations a_g on ground type A equal to 0.05*g*, 0.10*g*, 0.15*g*, 0.25*g* and 0.35*g*. Since the buildings were assumed to be founded on ground type B, seismic actions have been increased by the soil factor S, accounting for the influence of local ground conditions. The applied soil factor *S* was equal to 1.2 for the design seismic actions up to 0.15*gS*, 1.164 for 0.25*gS* and 1.076 for 0.35*gS*. Accounting also for the different design requirements corresponding to two different ductility classes, *i.e.*, medium (DCM) and high (DCH), 30 different bare frame types have been considered in total. The dimensions of all structural elements for the two-dimensional frame configurations are summarized in Table 2.

Furthermore, a group of three-dimensional prototype structures, representing typical 6-storey RC buildings having a storey height of 3.1 m, with spatial frame or wall-frame dual structural systems (Fig. 2a and Fig. 2b, respectively), has been considered.

Table 2 Beam and column dimensions of two-dimensional RC frame systems

a_g	Storey	3-storey DCM	3-storey DCH	6-storey DCM	6-storey DCH	9-storey DCM	9-storey DCH	
		Cross sectional width/height [*cm*]						
0.05g - 0.25g	1st - 3rd	35/35	35/35	45/45	45/45	55/55	55/55	External Columns
	4th - 6th	-	-	35/35	35/35	45/45	45/45	
	7th - 9th	-	-	-	-	35/35	35/35	
0.35g	1st - 3rd	45/45	35/35	50/50	45/45	60/60	55/55	
	4th - 6th	-	-	40/40	35/35	50/50	45/45	
	7th - 9th	-	-	-	-	40/40	35/35	
0.05g - 0.25g	1st	35/35	35/35	45/45	45/45	55/55	60/60	Internal Columns
	2nd - 3rd	35/35	35/35	45/45	45/45	55/55	55/55	
	4th - 6th	-	-	35/35	35/35	45/45	45/45	
	7th - 9th	-	-	-	-	35/35	35/35	
0.35g	1st	45/45	35/35	50/50	45/45	60/60	60/60	
	2nd - 3rd	45/45	35/35	50/50	45/45	60/60	55/55	
	4th - 6th	-	-	40/40	35/35	50/50	45/45	
	7th - 9th	-	-	-	-	40/40	35/35	
0.05g - 0.35g	1st - 3rd	45/24	30/40	50/24	30/45	55/24	30/50	Beams
	4th - 6th	-	-	50/24	30/45	55/24	30/50	
	7th - 9th	-	-	-	-	55/24	30/50	

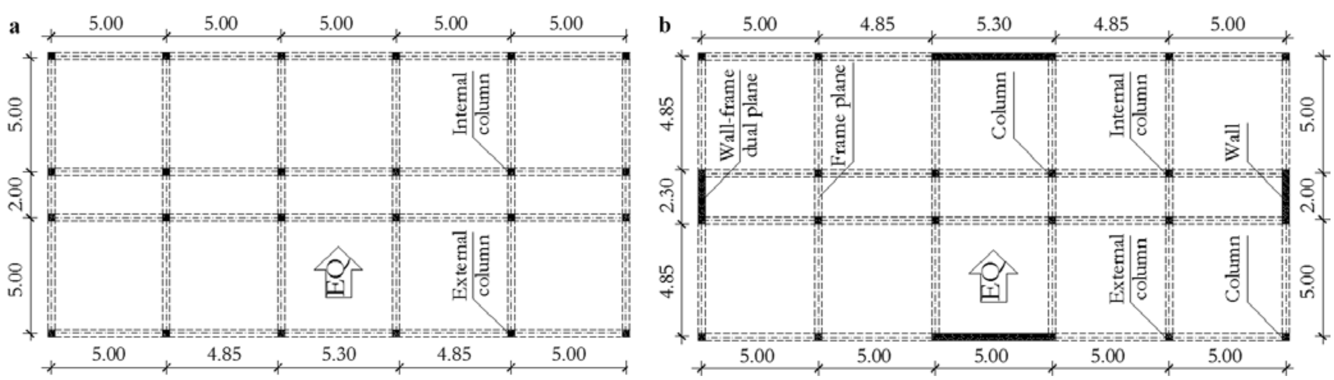

Figure 2. a) Masonry infill secant stiffness; b) Equivalent diagonal strut model

Each three-dimensional structural configuration has been designed for two levels of seismicity, corresponding to design peak ground accelerations a_g on ground type A equal to 0.25g and 0.35g. The design has also been accomplished for both ductility classes (DCM and DCH), resulting in eight different bare configurations, *i.e.*, four frame systems and four wall-frame dual systems. Dimensions of all structural elements for the three-dimensional frame and wall-frame dual systems are summarized in Table 3.

Table 3 Beam, column and wall dimensions of three-dimensional RC frame and wall-frame dual systems

Transversal direction			Frame planes DCM	Frame planes DCH			Frame planes DCM	Frame planes DCH		Wall-frame planes DCM	Wall-frame planes DCH	
a_g	Storey		Cross sectional width/height [*cm*]				Cross sectional width/height [*cm*]					
0.25g	1st - 3rd	**Frame system**	45/45	45/45	External Columns	**Wall-frame dual system**	45/45	45/45	External Columns	40/40	45/45	Columns
	4th - 6th		35/35	35/35			30/30	35/35		30/30	35/35	
0.35g	1st - 3rd		55/55	45/45			45/45	45/45		40/40	45/45	
	4th - 6th		45/45	35/35			30/30	35/35		30/30	35/35	
0.25g	1st - 3rd		45/45	45/45	Internal Columns		45/45	45/45	Internal Columns	30/230	30/230	Walls
	4th - 6th		35/35	35/35			30/30	35/35		30/230	30/230	
0.35g	1st - 3rd		55/55	45/45			45/45	45/45		30/230	30/230	
	4th - 6th		45/45	35/35			30/30	35/35		30/230	30/230	
0.25g - 0.35g	1st - 3rd		50/24	30/45	Beams		50/24	30/45	Beams	50/24	30/45	Beams
	4th - 6th		50/24	30/45			50/24	30/45		50/24	30/45	

3.3 Prototype masonry infill layouts

In addition to the bare structures, buildings with different infill layouts and masonry typologies have been analyzed, considering three characteristic, commonly adopted types of traditional unreinforced clay masonry. Typology T1 consists of a 8.0 cm thick single leaf masonry wall constructed of horizontally hollowed brick units with a 1.0 cm thick plaster on each face, typology T2 consists of two 12.0 cm thick leaves, each constructed of horizontally hollowed brick units divided by an intermediate 5.0 cm cavity and covered with a 1.0 cm thick plaster placed externally, while typology T3 is constituted by a single 30.0 cm thick leaf built with vertically hollowed brick units. Corresponding strength and stiffness properties, assumed based on experimental test [10], are summarized in Table 6, where E_{wh}, E_{wv} represent the secant modules of elasticity and f_{wh}, f_{wv} the values of compression strength for the horizontal and vertical direction, f_{wu} stands for the shear strength of the bed joints and f_{ws} for the shear strength under diagonal cracking.

Table 6 Properties of masonry for considered infill typologies

Typology	t_w $[mm]$	f_{wh} $[MPa]$	f_{wv} $[MPa]$	f_{wu} $[MPa]$	f_{ws} $[MPa]$	E_{wh} $[MPa]$	E_{wv} $[MPa]$
T1	100	1.18	2.02	0.44	0.55	991	1873
T2	260	1.11	1.50	0.25	0.31	991	1873
T3	300	1.50	3.51	0.30	0.36	1050	3240

To describe the infill deformation capacity, characteristic drifts $\delta_{m,j}$' equal to 0.30% and δ_u equal to 1.00% [6], corresponding to the attainment of damage limitation and ultimate limit state conditions, respectively, have been assumed for all infill typologies. The presence of infill T3 in all bays of a structural configuration is considered to represent a maximum infill density w_j = 100%, according to Equation (15) with reference properties $f_{w,0}$ = 0.30 MPa, $t_{w,0}$ = 300 mm. For all infilled structures, a constant infill distribution along the building height has been assumed.

$$w_j = \frac{\sum_{i=1}^{n_{b,j}} F_{w,i,j}}{f_{w,0} t_{w,0} \sum_{i=1}^{n_{b,j}} L_{w,i,j}} \tag{15}$$

Referring to two-dimensional frame structures, fully (F) and partially (P) infilled configurations, assuming the presence of infill only in the middle bay, have been included in the analyses. Considering all three infill typologies (T1, T2, and T3) for each structural configuration and infill layout, 180 two-dimensional infilled frames have been analyzed in total. For the case of three-dimensional frame and wall-frame dual structures, nonlinear analyses have been carried out for the transversal direction, considering, in addition to the bare structures, three different masonry infill distributions of typology T3. In particular, for each structural type, a fully (F) infilled configuration (w_j = 100%), with masonry infills in all bays of the transversal direction, and two intermediate cases, assuming $w_j \approx$ 60%, (P2; see Fig. 3a for frame system) and $w_j \approx$ 30% (P1; see Fig. 3b for wall-frame dual system), have been considered. Accordingly, 24 three-dimensional structural configurations with different infill layouts have been analyzed.

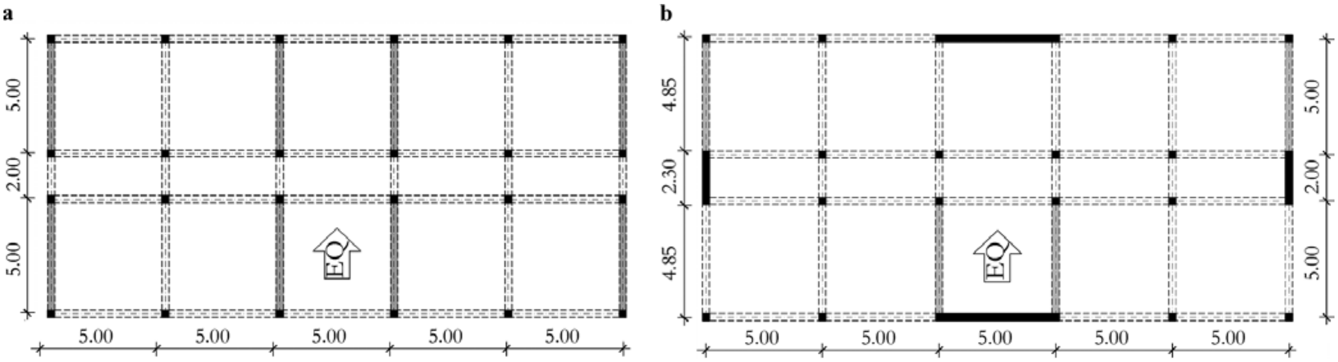

Figure 3. a) Masonry infill secant stiffness; b) Equivalent diagonal strut model

An overview of all considered structural configurations with different distributions and types of infill, as well as the corresponding infill density per storey w_j calculated from Equation (16), is given in Table 7.

Table 7 Summary of analyses performed on bare and infilled structures with corresponding infill density w_j

w_j [%]	Bare		Partial infill			Full infill	
	B	**P_T1**	**P_T2**	**P_T3**	**F_T1**	**F_T2**	**F_T3**
2d frame	0.0	8.2	12.1	16.7	48.9	72.2	100.0
	B		**P1_T3**	**P2_T3**			**F_T3**
3d frame	0.0		28.5	57.0			100.0
3d wall-frame	0.0		30.1	60.3			100.0

3.4 Resulting density-stiffness coefficients C_j

For the two-dimensional and three-dimensional structural configurations, fully infilled with typology T3, the total infill stiffness contribution has been assessed and the infill stiffness parameters $K_{I,j}$ have been evaluated according to Equation (3). Furthermore, average structural stiffness parameters $K_{S,j}$ have been calculated from Equation (9) for all structural configurations. Subsequently, the corresponding density-stiffness coefficients C_j have been determined according to Equation (14), as shown in Table 10 and Table 11, respectively, for the two-dimensional and three-dimensional structural configurations.

Table 10 Infill vs. structural stiffness ratios for two-dimensional frames fully infilled with infill T3 (F_T3)

C_j [-]		3-storey frame		6-storey frame		9-storey frame	
a_g	**Storey**	**DCM**	**DCH**	**DCM**	**DCH**	**DCM**	**DCH**
0.05g - 0.25g	1st	6.12	4.11	3.93	1.86	2.07	0.85
	2nd	9.45	5.11	7.38	2.58	4.09	1.43
	3rd	11.73	5.71	8.89	2.79	4.98	1.63
	4th	-	-	12.21	4.42	6.36	2.25
	5th	-	-	13.88	4.81	7.04	2.44
	6th	-	-	17.11	5.63	7.63	2.60
	7th	-	-	-	-	10.32	4.11
	8th	-	-	-	-	11.56	4.52
	9th	-	-	-	-	15.39	5.53
0.35g	1st	3.16	4.11	2.63	1.86	1.68	0.85
	2nd	5.64	5.11	4.97	2.58	3.44	1.43
	3rd	8.05	5.71	5.95	2.79	4.28	1.63
	4th	-	-	5.39	4.42	5.40	2.25
	5th	-	-	5.78	4.81	6.03	2.44
	6th	-	-	7.23	5.63	6.60	2.60
	7th	-	-	-	-	6.01	4.11
	8th	-	-	-	-	6.69	4.51
	9th	-	-	-	-	10.56	5.53

Table 11 Infill vs. structural stiffness ratios for three-dimensional frame and wall-frame dual systems fully infilled with infill T3 (F_T3) along the transversal direction

C_j [-]		6-storey frame		6-storey wall-frame dual system	
a_g	**Storey**	**DCM**	**DCH**	**DCM**	**DCH**
0.25g	1st	3.77	2.10	1.68	1.04
	2nd	6.94	3.12	3.92	2.15
	3rd	8.17	3.37	5.52	2.79
	4th	10.74	5.28	7.52	3.62
	5th	11.39	5.54	10.27	4.57
	6th	14.29	6.33	12.62	5.14
0.35g	1st	2.49	2.10	1.68	1.04
	2nd	5.09	3.12	3.92	2.15
	3rd	6.38	3.37	5.52	2.79
	4th	7.89	5.28	7.52	3.62
	5th	8.70	5.54	10.27	4.57
	6th	12.29	6.33	12.62	5.14

4. Correlation of in-plane drifts for bare and infilled RC structures

4.1 Results of nonlinear time-history analyses

For the needs of this study, average inter-storey drifts have been evaluated per storey, representing the average of maximum inter-storey drifts attained in each storey based on analyses for ten different records. Accordingly, for the different structural configurations and values of infill density w_j, pairs of average bare frame drifts $\delta_{\mu,j}$ and infilled frame drifts $\delta_{\mu,w,j}$ have been identified. Results obtained for the two-dimensional case study frame configurations at the damage limitation and the ultimate limit state for both ductility classes, fully infilled with different infill typologies (T1, T2 and T3), are shown in Fig. 4, Fig. 5 and Fig. 6, respectively. Each curve in these plots consists of five points, representing pairs of average bare frame and infilled frame drifts per storey, obtained for the same building configuration (*i.e.* 3-storey, 6-storey or 9-storey frame of ductility class M or H), designed for five different levels of seismicity (*i.e.* 0.05*gS*, 0.10*gS*, 0.15*gS*, 0.25*gS* and 0.35*gS*) at the corresponding intensity of seismic action. Similarly, the results for three-dimensional frame and wall-frame dual systems are shown in Fig. 7 and Fig. 8, respectively, at the damage limitation and the ultimate limit state for both ductility classes, with different T3 infill distributions (P1, P2 and F). Correspondingly, each curve in these plots consists of two points, representing pairs of drift per storey for bare and infilled structures, obtained for the same building configuration (*i.e.* 6-storey frame or wall-frame dual systems of ductility class M or H), designed for two different levels of seismicity (*i.e.* 0.25*gS* and 0.35*gS*) at the corresponding intensity of seismic action.

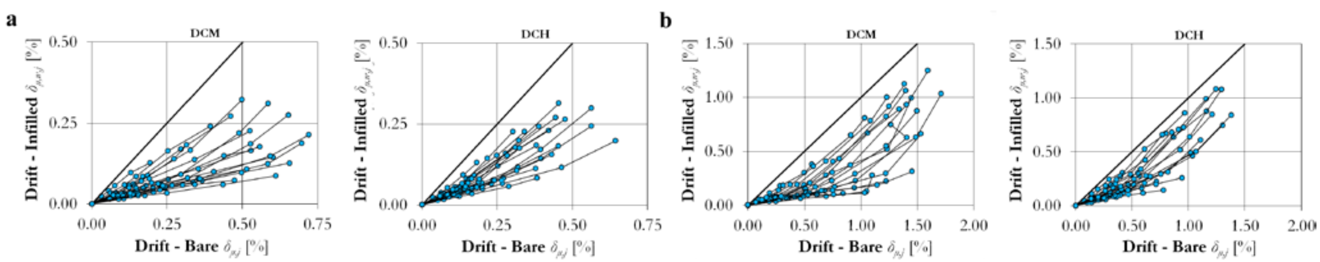

Figure 4. Average drift demands, 3-storey, 6-storey & 9-storey 2d frames (F_T1): a) DLS; b) ULS

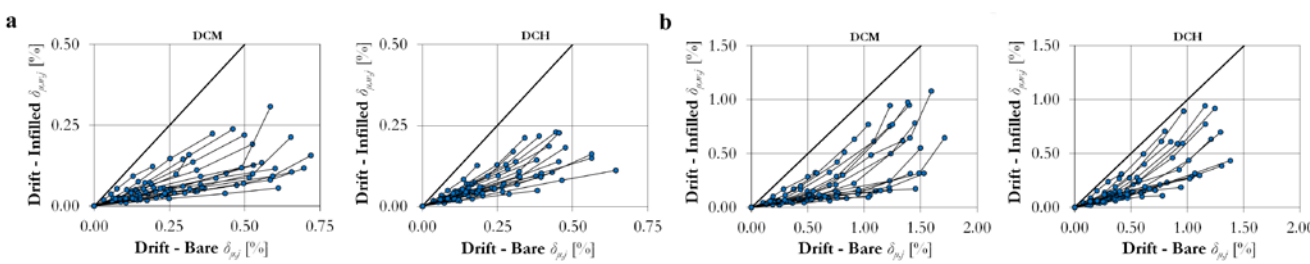

Figure 5. Average drift demands, 3-storey, 6-storey & 9-storey 2d frames (F_T2): a) DLS; b) ULS

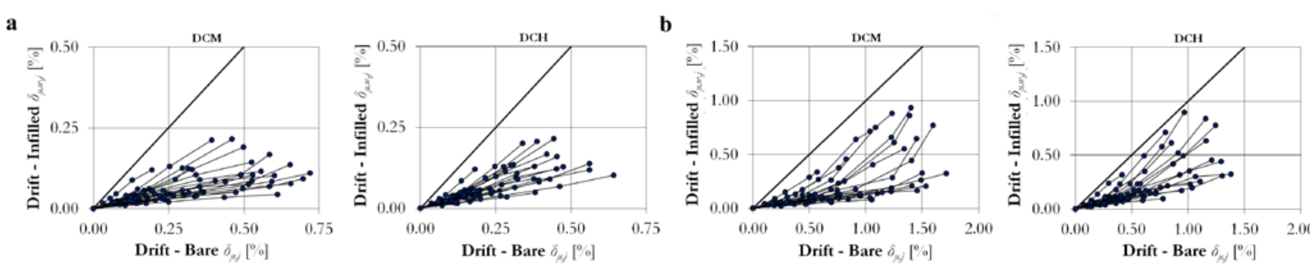

Figure 6. Average drift demands, 3-storey, 6-storey & 9-storey 2d frames (F_T3): a) DLS; b) ULS

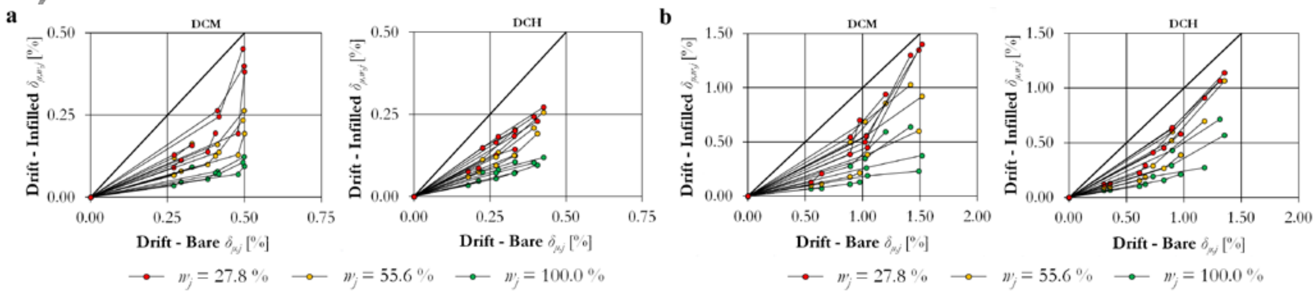

Figure 7. Average drift demands, 6-storey 3d frames (P1_T3, P2_T3 & F_T3): a) DLS; b) ULS

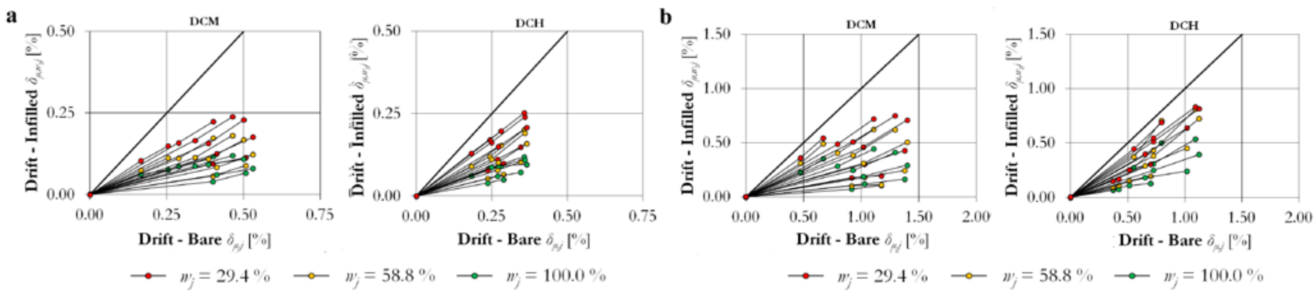

Figure 8. Average drift demands, 6-storey 3d wall-frames (P1_T3, P2_T3 & F_T3): a) DLS; b) ULS

Hence, one curve represents the relation between average drifts of bare and infilled structures in storey j of a building typology with infill density w_j (j = 1...n_s), designed for increasing levels of seismicity in ductility class M or H. The dimensions of RC structural elements of two-dimensional frame configurations and three-dimensional frame and wall-frame dual systems result to be the same for different design seismic intensities, resulting in the same structural stiffness, with exception of the columns in the frame structures designed for DCM at 0.35gS. Therefore, representing every infill typology and/or infill layout through the infill strength and stiffness parameter $K_{I,j}$, each of the presented curves can be associated with one value of the density-stiffness coefficient C_j, given by Equation (14). According to the results, the coefficient C_j can quantify the fact that stronger and more densely distributed infills cause a more pronounced reduction of drift demands of the infilled structure with respect to the bare frame; and similarly, that stiffer structural systems are less influenced by the presence of infills than more flexible configurations.

4.2 Simplified evaluation of drift demands for infilled configurations

Based on the presented results of parametric nonlinear time-history analyses, a simplified relationship can be introduced for the evaluation of maximum expected average inter-storey drift demands of masonry infilled structural configurations, in function of the average drift demand of corresponding bare structures. In particular, the inter-storey drift demand $\delta_{w,j}$ of the infilled configuration, described by the density-stiffness parameter $K_{I,j}$ in storey j given by Equation (3) of a RC structure represented by the stiffness parameter $K_{S,j}$ in storey j given by Equation (9) can be estimated in function of the density-stiffness coefficient C_j according to Equation (14), see also Table 10, and the drift demand δ_j of the corresponding bare configuration.

As illustrated in Figure 9a for C_j equal to 1.0 and in Figure 9b for different values of C_j, such correlation can be expressed using a bilinear curve, given by Equation (16), where $\delta_{m,j}$' is the inter-storey drift capacity for the masonry infills in storey j and the parameter δ_C defines the relation of drifts between bare and infilled configurations for C_j equal to 1.0.

$$\delta_{w,j} = \begin{cases} \dfrac{\delta_{m,j}'\delta_j}{\delta_{m,j}'+\delta_C C_j}, & \delta_j \le \delta_{m,j}'+\delta_C C_j \\ \delta_j - \delta_C C_j, & \delta_j > \delta_{m,j}'+\delta_C C_j \end{cases} \tag{16}$$

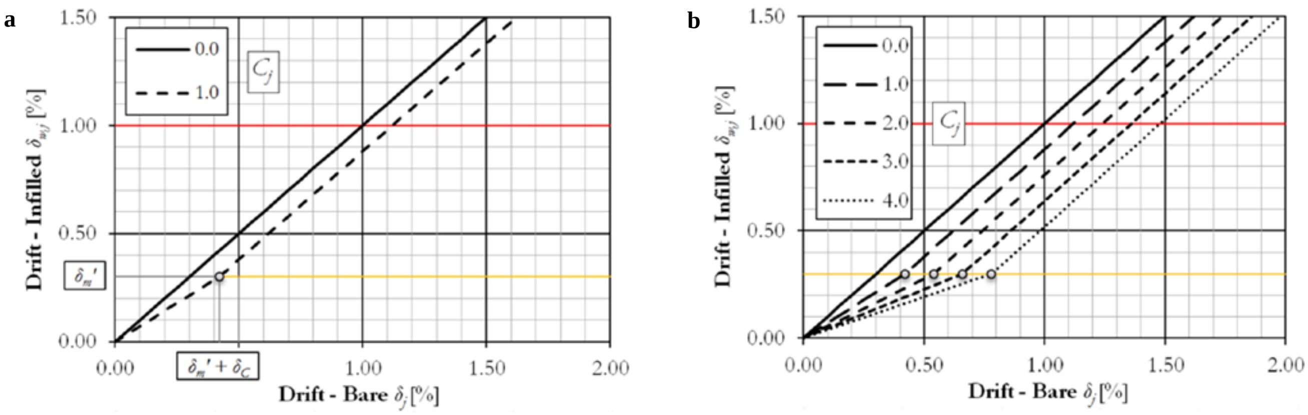

Figure 9. a) Relation of inter-storey drifts for bare (δ_j) and infilled ($\delta_{w,j}$) structures in function of density-stiffness coefficient C_j: a) Definition of bilinear curve for C_j = 1.0; b) Variation of bilinear curve for different values of C_j

The relationship allows a safe-sided approximation of expected inter-storey drift demands for infilled configurations, ensuring that upper-bound values are obtained. Hence, it can be adopted that the value of inter-storey drift capacity $\delta_{m,j}$ is equivalent to the allowable drift limit δ_{DLS} assigned to the exceedance of damage limitation limit state performance requirements. For a corresponding value of δ_C equal to 2/5 $\delta_{m,j}$' the bilinear curve in function of C_j has been found to describe reasonably the average drift demands obtained based on nonlinear analyses. By definition, according to Equation (16), for the corner point of the bilinear curve the drift of the infilled configuration $\delta_{w,j}$ always corresponds to the inter-storey drift capacity $\delta_{m,j}$', while the related bare frame drifts δ_j change depending on the parameter C_j. Notably, a value of C_j equal to zero actually corresponds to the bare structural configuration, while increasing values of C_j are obtained for stronger infill typologies, due to higher values of infill strength and/or thickness, as well as for building layouts with more densely distributed infills. Analogously, buildings with stiffer load-bearing structural systems are represented by smaller values of C_j. Further details regarding the validation of the proposed relationship between drift demands of bare and infilled structural configurations in function of the density-stiffness coefficient C_j given by Equation (14) can be found in [15].

5. Conclusions

The proposed correlation of displacement response allows the simplified evaluation of demands for infilled RC structures and may facilitate the effective design verification of inter-storey drift limits aimed at the achievement of a satisfactory infill response. In particular, with the aim of ensuring sufficient masonry infill damage control for masonry infills built in full contact with the surrounding RC structure, the verification of inter-storey drifts corresponding to infilled structures, rather than bare structural configurations, can be accomplished at the relevant limit states. At the same time, analyses carried out to accomplish the required verifications in the design of masonry infilled RC structures can still be performed considering bare configurations, without overly demanding additional considerations or computational efforts.

Accordingly, a practical approach to the verification of drift demands may be adopted in the design of regular RC structures with masonry infills, implementing for each storey *j* the following simple steps:

- Evaluate the inter-storey drift demand $\delta_{j,DLS}$ and $\delta_{j,ULS}$ of the bare structure based on commonly adopted methods of structural analysis.

- Calculate the infill strength and stiffness coefficient $K_{I,j}$ based on the given infill layout and the deformation capacity $\delta_{m,j}$' of infill typologies to be adopted, see Equation (2) and (3).

- Calculate the stiffness coefficient $K_{S,j}$ of the bare structure based on selected dimensions of structural elements, see Equation (9).

- Determine the corresponding density-stiffness coefficients C_j, see Equation (14).

- Establish the relationship between drift demands for bare and infilled structural configurations, see Equation (16) and calculate the inter-storey drift demands of the infilled configuration $\delta_{w,j,DLS}$ and $\delta_{w,j,ULS}$.

- Verify the inter-storey drift demands of the infilled configuration $\delta_{w,j,DLS}$ and $\delta_{w,j,ULS}$ against allowable values δ_{DLS} and δ_{ULS}, which reflect the acceptable levels of infill damage.

6. References

[1] Braga F, Manfredi V, Masi A., Salvatori A, Vona M (2011): Performance of non-structural elements in RC buildings during the L'Aquila, 2009 earthquake. *Bulletin of Earthquake Engineering* **9,** 307-324.

[2] Magenes G, Bracchi S, Graziotti F, Mandirola M, Manzini CF, Morandi P, Palmieri M, Penna A, Rosti A, Rota M, Tondelli M (2012): *Preliminary damage survey to masonry structures after the May 2012 Emilia earthquakes* v.1. (available at http://www.eqclearinghouse.org).

[3] Hermanns L, Fraile A, Alarcón E, Álvarez R (2014): Performance of buildings with masonry infill walls during the 2011 Lorca earthquake. *Bulletin of Earthquake Engineering* **12** (5), 1977-1997.

[4] Dolce M, Manfredi G (2009): Research needs in earthquake engineering highlighted by the 2009 l'Aquila earthquake in Manfredi, G., Dolce, M. (eds.) *The state of Earthquake Engineering Research in Italy*. ReLUIS-DPC 2005-2008 Project, 469-480.

[5] CEN (2004): Eurocode 8 - Design of structures for earthquake resistance, Part 1: General rules, seismic actions and rules for buildings, EN 1998-1, European Committee for Standardization, Brussels, Belgium.

[6] Hak S, Morandi P, Magenes G and Sullivan T (2012) Damage control for clay masonry infills in the design of RC frame structures. *Journal of Earthquake Engineering* **16** (S1), 1-35.

[7] Asteris PG, Antoniou ST, Sophianopoulos DS, Chrysostomou CZ (2011): Mathematical macromodeling of infilled frames: State of the art. *Journal of Structural Engineering* **137** (12), 1508-1517.

[8] Crisafulli FJ (1997): *Seismic behaviour of reinforced concrete structures with masonry infills*. PhD Dissertation, Department of Civil Engineering, University of Canterbury, New Zealand.

[9] Hak S, Morandi P, Magenes G (2013): Evaluation of infill strut properties based on in-plane cyclic tests. *Građevinar* **65** (6), 509-521.

[10] Calvi GM, Bolognini D (2001): Seismic response of RC frames infilled with weakly reinforced masonry panels. *Journal of Earthquake Engineering* **5** (2), 153-185.

[11] da Porto F, Guidi G, Dalla Benetta M, Verlato N (2012): *Sistemi costruttivi e risultati sperimentali*. Reluis Research Report (in Italian), University of Padova, Department of Civil and Environmental Engineering, Padova, Italy.

[12] Morandi P, Hak S, Magenes G (2014): In-plane Experimental Response of Strong Masonry Infills. *Proc. 9th International Masonry Conference*, Guimarães, Portugal.

[13] Decanini LD, Bertoldi SH, Gavarini C (1993): Telai tamponati soggetti ad azione sismica, un modello semplificato: confronto sperimentale e numerico. *Atti del VI convegno nazionale ANIDIS* (in Italian), Perugia, Italy.

[14] Kakaletsis DJ, Karayannis CG (2008): Influence of masonry strength and openings on infilled RC frames under cyclic loading. *Journal of Earthquake Engineering* **12**, 197-221.

[15] Stavridis A, Koutromanos I, Shing PB (2012): Shake-table tests of a three-story reinforced concrete frame with masonry infill walls. *Earthquake Engineering and Structural Dynamics* **41**(6), 1089–1108.

[16] Hak S, Morandi P, Magenes G (2016): Simplified evaluation of drifts for RC buildings with masonry infills. *Proc. 16th International Brick and Block Masonry Conference*, Padova, Italy.

[17] Morandi P, Hak S, Magenes G (2011): Comportamento sismico delle tamponature in laterizio in telai in c.a.: definizione dei livelli prestazionali e calibrazione di un modello numerico. *Atti del XIV convegno nazionale* ANIDIS (in Italian), Bari, Italy.

[18] Hak S, Morandi P, Magenes G (2013): Damage Control of Masonry Infills in Seismic Design. Report EUCENTRE 2013/01, IUSS Press, Pavia, Italy.